Research Article

Mohamed Abdelwahed* and Nejmeddine Chorfi

On the problem of detecting source points acting on a fluid

https://doi.org/10.1515/dema-2023-0108
received May 18, 2023; accepted August 31, 2023

Abstract: The detection problem of a finite number of source points acting on a steady incompressible fluid flow from overdetermined boundary data was studied. The approach used in this study deals with the topological sensitivity technique. An asymptotic analysis of a prescribed cost function with respect to the domain perturbation was developed. Some numerical results to illustrate the efficiency and robustness of the developed source point detection algorithm were presented.

Keywords: optimization, source point detection, topological sensitivity, Stokes equations

MSC 2020: 35Q30, 49Q10, 74P05

1 Introduction

Consider $\Omega \subset \mathbb{R}^2$, an open-bounded domain occupied by a stationary viscous incompressible fluid flow governed by the Stokes equations:

$$\begin{cases} -\nu\Delta u + \nabla p = F & \text{in } \Omega \\ \operatorname{div} u = 0 & \text{in } \Omega \\ u = u^* & \text{on } \Gamma, \end{cases} \tag{1}$$

where u is the fluid velocity, p is the pressure, ν is the kinematic viscosity, u^* is a given boundary velocity on the boundary $\Gamma = \partial\Omega$, and

$$F = \sum_{i=1}^{N} \mathcal{F}_i \delta_{x_i}$$

is a source term representing the total action of a finite number of particles, where δ_{x_i} represents the Dirac function at $x_i \in \Omega$ and $\mathcal{F}_i$ is a constant source point force. We suppose that a given other boundary condition $\sigma(u, p)n = \phi$ on the stress tensor, $\sigma(u, p) = -pI + \mu(\nabla u + \nabla u^T)$ is given on Γ, where I denotes the 2×2 identity matrix and n is the unit normal vector along the boundary Γ.

The aim is to identify the unknown source points [1]. Such a problem can be motivated by the study of the flow near colloidal particle phenomena [2,3]. This problem has been studied in [4] using a game strategy approach.

Our purpose is to use the topological sensitivity analysis method [5–11] associated with Kohn-Vogelius formulation [12–15] to solve this problem. We begin in Section 2 by the state of the detection point source inverse problem. Section 3 is devoted to the asymptotic development analysis based on the topological

*** Corresponding author: Mohamed Abdelwahed,** Department of Mathematics, College of Sciences, King Saud University, Riyadh, Saudi Arabia, e-mail: mabdelwahed@ksu.edu.sa
Nejmeddine Chorfi: Department of Mathematics, College of Sciences, King Saud University, Riyadh, Saudi Arabia, e-mail: nchorfi@ksu.edu.sa

sensitivity method. In Section 4, an iterative algorithm based on the developed approach is presented. Finally, some two- and three-dimensional numerical tests are presented in Section 5 to illustrate the efficiency of the presented algorithm.

2 Detection of source point problem

2.1 Direct problem

The direct problem consists in studying the action of source points on a viscous incompressible fluid described by the Stokes equations (1).

Because of the divergence-free condition, we suppose that u^* satisfies the following compatibility condition:

$$\int_{\Gamma} u^*.\, n\mathrm{d}s = 0. \tag{2}$$

To discuss the well-posedness of the direct problem, we introduce the fundamental solution (E, P) of the Stokes equations in the two-dimensional case

$$E(y) = \frac{1}{4\pi\nu} - (\log(r)I + e_r e_r^T) \quad \textit{and} \quad P(y) = \frac{y}{2\pi r^2},$$

with $r = \|y\|$, $e_r = y/r$, and e_r^T is the transposed vector of e_r.

The solution (u, p) to (1) can be decomposed as:

$$u = u_s + u_r \quad \textit{and} \quad p = p_s + p_r,$$

where (u_s, p_s) is a function with a finite number of singularities coinciding with the locations of the source points. It is the solution to:

$$\begin{cases} -\nu\Delta u_s + \nabla p_s = \sum_{i=1}^{N} \mathcal{F}_i \delta_{x_i} \text{ in } \mathbb{R}^2, \\ \text{div } u_s = 0 \qquad \text{in } \mathbb{R}^2. \end{cases} \tag{3}$$

The second part (u_r, p_r) is a regular function solution to:

$$\begin{cases} -\nu\Delta u_r + \nabla p_r = 0 \qquad \text{in } \Omega, \\ \text{div } u_r = 0 \qquad \text{in } \Omega, \\ u_r = u^* - v_s \text{ on } \Gamma. \end{cases} \tag{4}$$

We have the following result ([16,17] for the proof).

Theorem 2.1. *Suppose that the boundary* Γ *is of class* C^m, $m \geq 1$. *If* $u^* \in H^{m-1/2}(\Gamma)$ *verifying* (2), *then Problem* (1) *admits a unique solution* (u, p) *satisfying*

$$u = u_s + u_r \quad \textit{and} \quad p = p_s + p_r,$$

with (u_s, p_s) *solution to* (3), *given by*:

$$u_s = \sum_{i=1}^{N} U(.-x_i)\mathcal{F}_i \quad \textit{and} \quad p_s = \sum_{i=1}^{N} P(.-x_i).\, \mathcal{F}_i,$$

and $(u_r, p_r) \in H^m(\Omega) \times H^{m-1}(\Omega)$ *solution to* (4).

2.2 Inverse problem

The inverse problem consists in finding the number N and detecting the source point locations x_i using measurement of the stress tensor $\sigma(u,p).\ n$ on the boundary Γ. The following theorem gives an identifiability result (see [12] for the proof).

Theorem 2.2. *Let* (u_k, p_k), $k = 1, 2$, *be the solutions to*:

$$\begin{cases} -\nu\Delta u_k + \nabla p_k = \sum_{i=1}^{N^k} \mathcal{F}_i^k \delta_{x_i^k} \ in\ \Omega, \\ \quad \text{div}\ u_k = 0 \qquad in\ \Omega, \\ \quad u_k = u^* \qquad on\ \Gamma. \end{cases}$$

Then, if $\sigma(u_1,p_1)\cdot n_{|\Gamma} = \sigma(u_2,p_2)\cdot n_{|\Gamma}$, *we have*

$$N^1 = N^2 = N, \quad \mathcal{F}_i^1 = \mathcal{F}_i^2, \quad x_i^1 = x_i^2, \quad \text{and} \quad i = 1,\dots,N.$$

We conclude that using Theorem 3.1, the number and locations of source points are uniquely determined by a single measurement of the stress tensor $\sigma(u,p).\ n$ on the boundary Γ.

3 Topological sensitivity approach

3.1 Variation of the cost function with respect to small topological perturbation

3.1.1 General results

For $1 \le p < 2$, let

$$\begin{array}{rcl} \mathcal{G} : L^p(\Omega)^2 & \to & \mathbb{R} \\ f & \mapsto & \mathcal{G}(f) \end{array} \tag{5}$$

be a differentiable functional on $L^p(\Omega)^2$. We have

$$\nabla\mathcal{G}(f)\delta f = \int_\Omega \mathcal{R}(x)\delta f(x)\mathrm{d}x,\ \forall \delta f \in L^p(\Omega)^2, \tag{6}$$

where $\mathcal{R}$ denotes the Riesz representative of the differential $\nabla\mathcal{G}(f)$. We want to study the variation of the functional $\mathcal{G}$ with respect to a finite topological perturbation of f on the form:

$$\delta f_\varepsilon(x) = \begin{cases} \mathcal{F} & \text{if } x \in \varpi_\varepsilon, \\ 0 & \text{if } x \in \Omega\backslash\overline{\varpi_\varepsilon}, \end{cases} \tag{7}$$

where $\mathcal{F} \in \mathbb{R}^2$ is a constant vector and ϖ_ε is a geometry perturbation of size $\varepsilon > 0$ small enough.

We make the following assumptions.

Hypothesis 3.1

- The function $\mathcal{G}$ is differentiable, and there exists constant $\gamma_1 > 0$ such that

$$\text{for all } f \in L^p(\Omega)^2, \quad |\mathcal{G}(f+\delta f) - \mathcal{G}(f) - \nabla\mathcal{G}(f)\delta f| \le \gamma_1 \|\delta f\|^2_{L^p(\Omega)^2}, \quad \forall \delta f \in L^p(\Omega)^2. \tag{8}$$

- The function $\mathcal{R}$ is Lipschitz continuous, i.e., there exists a constant $\gamma_2 > 0$ such that

$$\|\mathcal{R}(x) - \mathcal{R}(y)\| \le \gamma_2\|x-y\|, \quad \forall x, y \in \Omega. \tag{9}$$

The following theorem gives the variation of $\mathcal{G}$.

Theorem 3.1. *If Hypothesis* 3.1 *holds, we have*

$$\mathcal{G}(f + \delta f_\varepsilon) - \mathcal{G}(f) = \rho(\varepsilon)\{\mathcal{F} \cdot \mathcal{R}(x_0)\} + o(\rho(\varepsilon)), \tag{10}$$

where $\rho(\varepsilon) = \text{meas}(\varpi_\varepsilon)$.

Proof. First, we have

$$|\mathcal{G}(f + \delta f_\varepsilon) - \mathcal{G}(f) - \rho(\varepsilon)\mathcal{F} \cdot \mathcal{R}(x_0)| \le |\mathcal{G}(f + \delta f_\varepsilon) - \mathcal{G}(f) - \nabla\mathcal{G}(f)\delta f_\varepsilon| + |\nabla\mathcal{G}(f)\delta f_\varepsilon - \rho(\varepsilon)\,\mathcal{F} \cdot \mathcal{R}(x_0)|. \tag{11}$$

Thanks to (8), we derive

$$|\mathcal{G}(f + \delta f_\varepsilon) - \mathcal{G}(f) - \nabla\mathcal{G}(f)\delta f_\varepsilon| \le \gamma_1 \|\delta f_\varepsilon\|^2_{L^p(\Omega)^2}.$$

Using (7) and the fact that $p < 2$, we obtain

$$\|\delta f_\varepsilon\|^2_{L^p(\Omega)^2} \le c(\rho(\varepsilon)^{1/p})^2 = c\rho(\varepsilon)^{2/p} = o(\rho(\varepsilon)).$$

Therefore,

$$|\mathcal{G}(f + \delta f_\varepsilon) - \mathcal{G}(f) - \nabla\mathcal{G}(f)\delta f_\varepsilon| = o(\rho(\varepsilon)). \tag{12}$$

For the second part in (11), we have

$$\left|\int_\Omega \mathcal{R}(x)\cdot\,\delta f_\varepsilon(x)\mathrm{d}x - \rho(\varepsilon)\mathcal{F} \cdot \mathcal{R}(x_0)\right| = \left|\int_\Omega (\mathcal{R}(x) - \mathcal{R}(x_0))\cdot\delta f_\varepsilon(x)\mathrm{d}x\right|.$$

It follows from (9) that

$$\left|\int_\Omega \mathcal{R}(x)\delta f_\varepsilon(x)\mathrm{d}x - \rho(\varepsilon)\mathcal{F} \cdot \mathcal{R}(x_0)\right| \le \gamma_2\int_\Omega \|x - x_0\|\|\delta f_\varepsilon(x)\|\mathrm{d}x = \gamma_2\|\mathcal{F}\|\int_{\varpi_\varepsilon} \|x - x_0\|\mathrm{d}x \le \gamma_2\|\mathcal{F}\|\varepsilon\rho(\varepsilon). \tag{13}$$

Finally, using (12) and (13), we deduce the desired result. □

3.1.2 Perturbation of the Stokes problem

Consider now the Stokes problem case:

$$\begin{cases} -\nu\Delta u + \nabla p = F & \text{in } \Omega, \\ \quad \text{div } u = 0 & \text{in } \Omega, \\ \quad\quad u = u^* & \text{on } \Gamma. \end{cases} \tag{14}$$

For all $F \in L^2(\Omega)$ and $u^* \in H^{1/2}(\Gamma)$, Problem (14) has one solution $(u, p) \in H^1(\Omega) \times L^2_0(\Omega)$. For more details and proof, one may consult [18] or [17].

Using a weak formulation of the previous system, one can show that u is the solution to the following variational problem:

$$\begin{cases} u \in \mathcal{V}, \\ \mathcal{A}(u, w) = L(w), \ \ \forall w \in \mathcal{V}^0, \\ u = u^* \text{ on } \Gamma, \end{cases}$$

with

$$\begin{aligned}\mathcal{V} &= \{w \in H^1(\Omega),\ \text{div}\ w = 0\},\\ \mathcal{V}^0 &= \{w \in \mathcal{V},\quad w_{|\Gamma} = 0\},\\ \mathcal{A}(v,w) &= \nu \int_\Omega \nabla v\ \nabla w \mathrm{d}x,\quad \forall v, w \in \mathcal{V},\\ L(w) &= \int_\Omega F w \mathrm{d}x,\quad \forall w \in \mathcal{V}.\end{aligned}$$

Obviously, $\mathcal{A}$ is a continuous bilinear form on $\mathcal{V} \times \mathcal{V}$ and L is a continuous linear form on $\mathcal{V}$.

For all $f \in L^p(\Omega)^2$, we denote by L_f the following linear form:

$$\begin{aligned}L_f : \mathcal{V} &\longrightarrow \mathbb{R}\\ w &\longmapsto L_f(w) = L(w) + \int_\Omega f(x) w(x) \mathrm{d}x.\end{aligned}$$

We have the following lemma.

Lemma 3.1. *The map*

$$\begin{aligned}L^p(\Omega)^2 &\longrightarrow \mathcal{L}(\mathcal{V})\\ f &\longmapsto L_f\end{aligned} \tag{15}$$

is continuous for $p > 1$.

Proof. Thanks to [19] (Theorem IX.16), we know that $H^1(\Omega) \subset L^q(\Omega)$ for $1 \le q < +\infty$. It is well known that if $v \in L^{p_1}(\Omega)$ and $w \in L^{p_2}(\Omega)$, the product $v \cdot w \in L^p(\Omega)$ with $\frac{1}{p} = \frac{1}{p_1} + \frac{1}{p_2}$.

Consequently, the map $f \mapsto L_f$ is continuous as soon as

$$\frac{1}{p} + \frac{1}{q} = 1. \tag{16}$$

Then, combining equation (16) and the conditions on q for which we have $H^1(\Omega) \subset L^q(\Omega)$, we deduce that the map is continuous for $p > 1$. □

In the following, we denote by $u_f \in \mathcal{V}$ the unique solution of the following variational problem:

$$\mathcal{A}(u_f, w) = L_f(w) \quad \forall w \in \mathcal{V}^0, \tag{17}$$

and we consider the cost function $\mathcal{G}$ defined by:

$$\begin{aligned}\mathcal{G}:\ L^p(\Omega)^2 &\longrightarrow \mathbb{R}\\ f &\longmapsto \mathcal{G}(f) = J(u_f),\end{aligned} \tag{18}$$

where J is a given functional defined on Ω.

If J is differentiable, using the Lagrangian method, one can prove that the function $\mathcal{G}$ is differentiable and we have

$$\nabla \mathcal{G}(f)\delta f = -\int_\Omega \delta f(x).\ v_f(x) \mathrm{d}x,\quad \forall \delta f \in L^p(\Omega)^2, \tag{19}$$

where $v_f \in \mathcal{V}^0$ is the solution to the associated adjoint problem:

$$\mathcal{A}(w, v_f) = -DJ(u_f)w,\quad \forall w \in \mathcal{V}^0. \tag{20}$$

Relations (6) and (19) involve that

$$\mathcal{R} = -v_f. \tag{21}$$

We note that the regularity of $\mathcal{R}$ depends on that of the functional J.

Let us consider now the following particular case:

$$f \equiv 0, \quad \text{and} \quad \delta f = \delta f_\varepsilon.$$

Posing $j(\varepsilon) = J(u_\varepsilon)$, where u_ε is the solution $u_{0+\delta f_\varepsilon}$. We deduce the following result using Theorem 3.1.

Proposition 3.1. *The cost function j has the following asymptotic expansion*:

$$j(\varepsilon) - j(0) = \rho(\varepsilon)\,\{-\mathcal{F}.\, v_0\}(x_0) + o(\rho(\varepsilon)). \tag{22}$$

3.2 Cost function examples

We now discuss Hypothesis 3.1. We consider the standard example of a cost function that we will use in numerical tests:

$$J(u) = \int_\Omega |u - \mathcal{U}|^2 \mathrm{d}x, \tag{23}$$

where $\mathcal{U} \in H^1(\Omega)$.

Proposition 3.2. *The cost function* (23) *satisfies Hypothesis* 3.1 *with*

$$\nabla\mathcal{G}(f)(\delta f) = \int_\Omega v_f.\, \delta f \mathrm{d}x, \quad \forall \delta f \in L^p(\Omega)^2,$$

with $v_f \in \mathcal{V}^0$ *solution to the following adjoint problem*:

$$\mathcal{A}(w, v_f) = -2\int_\Omega (u_f - \mathcal{U})w \mathrm{d}x, \quad \forall w \in \mathcal{V}^0.$$

Proof. It is easy to show that J is differentiable on $\mathcal{V}$ and we have

$$DJ(u)w = 2\int_\Omega (u - \mathcal{U}).\, w \mathrm{d}x, \quad \forall w \in \mathcal{V}.$$

Then, the adjoint solution v_f is the solution to:

$$\begin{cases} v_f \in \mathcal{V}^0, \\ \mathcal{A}(w, v_f) = -2\int_\Omega (u_f - \mathcal{U})w \mathrm{d}x, \quad \forall w \in \mathcal{V}^0. \end{cases} \tag{24}$$

Using (18), (19), and (23), we obtain

$$\begin{aligned} \mathcal{G}(f + \delta f) - \mathcal{G}(f) - \nabla\mathcal{G}(f)\delta f &= \int_\Omega |u_{f+\delta f} - \mathcal{U}|^2 \mathrm{d}x - \int_\Omega |u_f - \mathcal{U}|^2 \mathrm{d}x - \int_\Omega v_f \cdot \delta f \mathrm{d}x \\ &= 2\int_\Omega (u_f - \mathcal{U}).\, (u_{f+\delta f} - u_f)\mathrm{d}x + \|u_{f+\delta f} - u_f\|^2_{0,\Omega} - \int_\Omega v_f \cdot \delta f \mathrm{d}x. \end{aligned} \tag{25}$$

Recall that $u_f \in \mathcal{V}$ is the solution to:

$$\begin{cases} \mathcal{A}(u_f, w) = L_f(w), \quad \forall w \in \mathcal{V}, \\ u = u^* \text{ on } \Gamma. \end{cases} \tag{26}$$

Then, $(u_{f+\delta f} - u_f) \in \mathcal{V}^0$ satisfies

$$\mathcal{A}(u_{f+\delta f} - u_f, w) = \int_\Omega \delta f \cdot w \mathrm{d}x, \quad \forall w \in \mathcal{V}^0. \tag{27}$$

Choosing $w = u_{f+\delta f} - u_f$ in (24) and $w = v_f$ in (27), we deduce

$$2\int_\Omega (u_f - \mathcal{U}).\,(u_{f+\delta f} - u_f)\mathrm{d}x = \int_\Omega \delta f \cdot v_f \mathrm{d}x.$$

Hence,

$$\mathcal{G}(f + \delta f) - \mathcal{G}(f) - \nabla\mathcal{G}(f)\delta f = \|u_{f+\delta f} - u_f\|^2_{0,\Omega}. \tag{28}$$

To estimate the term $\|u_{f+\delta f} - u_f\|^2_{0,\Omega}$, we need to suppose that the perturbation δf has the form:

$$\delta f(x) = \begin{cases} \mathcal{F}, & \text{if } x \in \varpi_\varepsilon, \\ 0, & \text{if } x \in \Omega \backslash \overline{\varpi_\varepsilon}, \end{cases}$$

where $\mathcal{F} \in \mathbb{R}^2$ is a constant vector and $\varepsilon > 0$ is small enough.

Posing $w_f = u_{f+\delta f} - u_f$ and $s_f = p_{f+\delta f} - p_f$, then $(w_f, s_f) \in H^1_0(\Omega) \times L^2_0(\Omega)$ is the solution to:

$$\begin{cases} -\nu\Delta w_f + \nabla s_f = \delta f \text{ in } \Omega, \\ \quad \text{div } w_f = 0 \quad \text{in } \Omega, \\ \quad\quad w_f = 0 \quad \text{on } \Gamma. \end{cases}$$

Then, there exists a positive constant c, independent of f, such that

$$\|w_f\|^2_{1,\Omega} \le c\int_\Omega \delta f.\, w_f \mathrm{d}x.$$

We choose $p = 13/10$ and $q = 13/3$. Using the Holder inequality and the Sobolev embedding theorem, we derive

$$\int_\Omega \delta f \cdot w_f \mathrm{d}x \le \|\delta f\|_{L^{13/10}(\varpi_\varepsilon)} \|w_f\|_{L^{13/3}(\Omega)} = c\rho(\varepsilon)^{10/13}\|w_f\|_{1,\Omega}.$$

Hence,

$$\|u_{f+\delta f} - u_f\|^2_{0,\Omega} = \|w_f\|^2_{1,\Omega} = o(\rho(\varepsilon)). \tag{29}$$

Using (28) and (29), we deduce

$$\mathcal{G}(f + \delta f) - \mathcal{G}(f) - \nabla\mathcal{G}(f)\delta f = o(\rho(\varepsilon)).$$

□

4 Numerical algorithm

As an application of the previous theoretical results, we use Formula (22) to detect locations, intensity, and number of source points acting on fluid governed by the Stokes equations.

Let Ω be a two-dimensional domain occupied by the fluid containing some source points $S = \{s_i = (X_i, \mathcal{F}_i), 1 \le i \le N_S\}$, where X_i and $\mathcal{F}_i$ denote, respectively, the position and intensity of the source point i and N_s the total source point number.

Our aim is to identify S using a boundary measurement ϕ of the stress tensor.

4.1 The inverse problem

The inverse problem that we consider can be formulated as follows:

Given u^* a velocity on the boundary Γ, satisfying the compatibility Condition (2), find the set of source points S such that the solution (u^s, p^s) to

$$\begin{cases} -\nu\Delta u^s + \nabla p^s = \sum_{i=1}^{N_s} \mathcal{F}_i \delta_{X_i} & \text{in } \Omega, \\ \operatorname{div} u^s = 0 & \text{in } \Omega, \\ u^s = u^* & \text{on } \Gamma \end{cases}$$

satisfies $\sigma(u^s, p^s)n_{|\Gamma} = \phi$.

4.2 The cost function

Since the boundary condition is overspecified, we use the Kohn-Vogelius criterion:

$$j(S) = J(u_D^s, u_N^s) = \int_\Omega |u_D^s - u_N^s|^2 \mathrm{d}x,$$

where (u_D^s, p_D^s) is the solution to the Stokes equations with the Dirichlet condition on Γ:

$$\begin{cases} -\nu\Delta u_D^s + \nabla p_D^s = \sum_{i=1}^{N_s} \mathcal{F}_i \delta_{X_i} & \text{in } \Omega, \\ \operatorname{div} u_D^s = 0 & \text{in } \Omega, \\ u_D^s = u^* & \text{on } \Gamma, \end{cases}$$

and (u_N^s, p_N^s) is solution to the Stokes equations with Neumann condition on Γ:

$$\begin{cases} -\nu\Delta u_N^s + \nabla p_N^s = \sum_{i=1}^{N_s} \mathcal{F}_i \delta_{X_i} & \text{in } \Omega, \\ \operatorname{div} u_N^s = 0 & \text{in } \Omega, \\ u_N^s = 0 & \text{on } \Gamma_1, \\ \sigma(u_N^s, p_N^s)n = \phi & \text{on } \Gamma. \end{cases}$$

We note that $\Gamma = \Gamma_1 \cup \Gamma_2$ with $\Gamma_1 \cap \Gamma_2 = \varnothing$ and u^* is equal to u_1 on Γ_1 and 0 on Γ_2.

4.3 Topological gradient

To compute the topological gradient, we need to solve the following problems:

- The two direct problems

$$\begin{cases} -\nu\Delta u_D + \nabla p_D = 0 & \text{in } \Omega, \\ \operatorname{div} u_D = 0 & \text{in } \Omega, \\ u_D = u^* & \text{on } \Gamma, \end{cases}$$
$$\begin{cases} -\nu\Delta u_N + \nabla p_N = 0 & \text{in } \Omega, \\ \operatorname{div} u_N = 0 & \text{in } \Omega, \\ u_N = 0 & \text{on } \Gamma_1, \\ \sigma(u_N, p_N)n = \phi & \text{on } \Gamma. \end{cases} \tag{30}$$

- The two adjoint problems

$$\begin{cases} -\nu\Delta v_D + \nabla q_D = -2(u_D - u_N) & \text{in } \Omega, \\ \operatorname{div} v_D = 0 & \text{in } \Omega, \\ v_D = 0 & \text{on } \Gamma, \end{cases}$$
$$\begin{cases} -\nu\Delta v_N + \nabla q_N = 2(u_D - u_N) & \text{in } \Omega, \\ \operatorname{div} v_N = 0 & \text{in } \Omega, \\ \sigma(v_N, v_N)\cdot \mathbf{n} = 0 & \text{on } \Gamma. \end{cases} \tag{31}$$

Using Proposition 3.1, the topological gradient is given by:

$$\delta j(x) = -\mathcal{F}\cdot\{v_D(x) + v_N(x)\}, \quad \forall x \in \Omega. \tag{32}$$

4.4 Algorithm

Our identification problem can be formulated as a topological optimization problem: find the optimal location of the disks $s_i = B(X_i, r_i)$ of center X_i and radius r_i, $1 \le i \le N$, inside the domain Ω minimizing the considered objective function. We propose, in this case, a multi-iteration process in the following sense:

At the first iteration, we keep only one force location corresponding to the "most negative" topological gradient. The next iteration repeats the same procedure in the new domain obtained after inserting the force detected during the previous iteration.

We use the following numerical algorithm:

- Initialization: choose $\Omega_0 = \Omega$, and set $k = 0$.
- Repeat until target is reached:
  - solve (30) and (31) in Ω_k,
  - compute the topological sensitivity δj_k given by (32),
  - set $\Omega_{k+1} = \{x \in \Omega_k, \quad \delta j_k(x) > c_{k+1}\}$ where c_{k+1} is the chosen constant,
  - $k \leftarrow k + 1$.

We propose an adaptation of the previous algorithm to our context. We consider the set:

$$\{x \in \Omega_k; \quad \delta j_k(x) < c_{k+1}\}.$$

Each connected component of this set is a neighborhood of a point source detected by the algorithm. In numerical computations, we have used $c_{k+1} = 0.8\kappa$, where κ is the most negative minimum of $\delta j_k(x)$.

In the aforementioned algorithm, Systems (30) and (31) are discretized by a finite element method. The numerical simulations are carried out using a developed 2D numerical software.

In practice, certain stopping criteria can be implemented successfully, such as the volume of material to remove [6], the number of the holes to insert [5], or the number of obstacles to detect [7]. In our case, we have imposed that the value of δj must be positive as a stopping criterion.

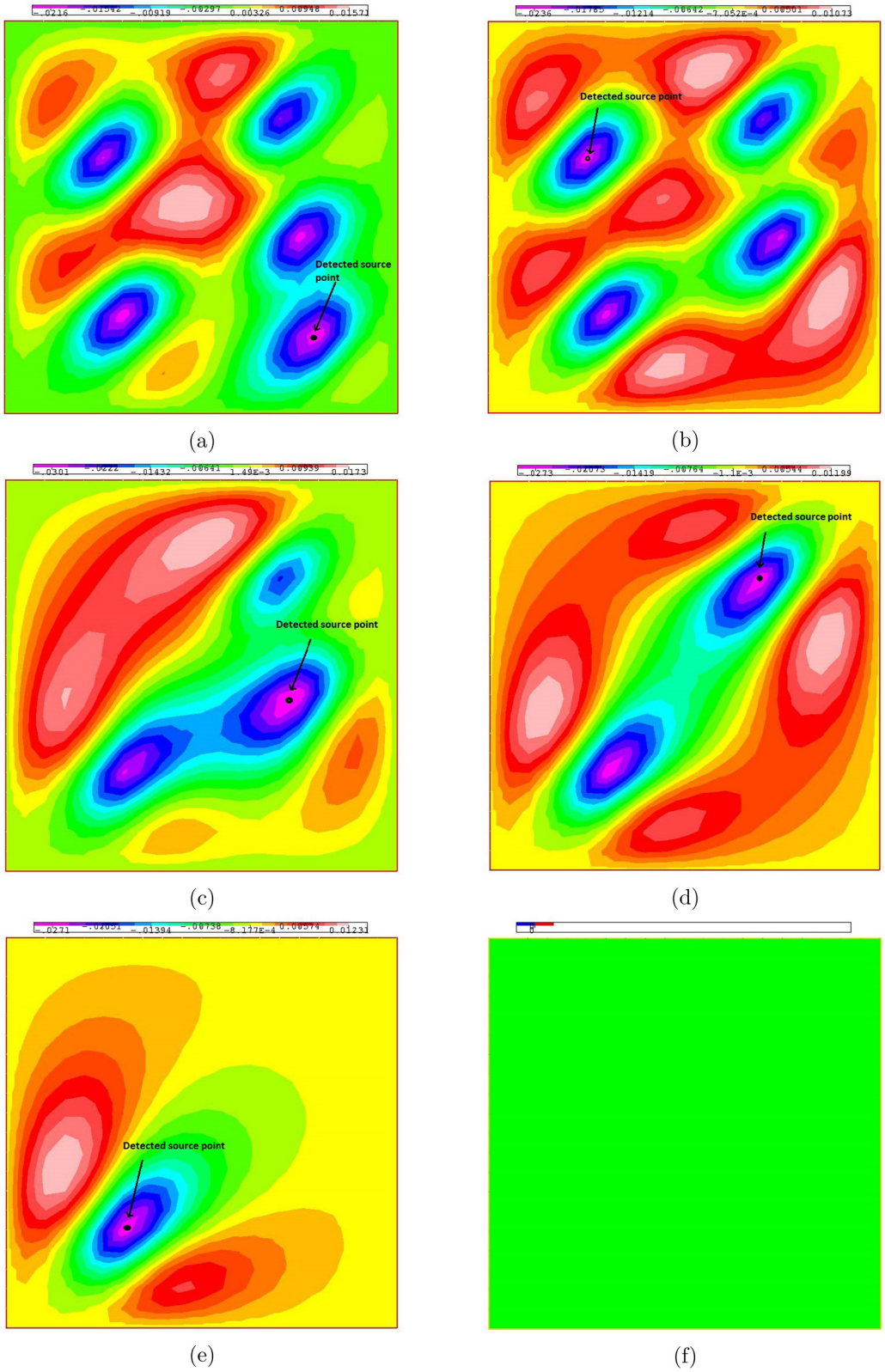

Figure 1: Isovalues of δj at each iteration showing the position of the detected source point (black dots) corresponding to the minimum found: (a) Iteration 1, (b) Iteration 2, (c) Iteration 3, (d) Iteration 4, (e) Iteration 5, and (f) Iteration 6.

5 Numerical tests

The numerical test concerns the detection of the optimal location of the well-separated source points in a two-dimensional case.

Consider $\Omega = [0,1] \times [0,1]$ a two-dimensional domain discretized by a non-uniform triangular mesh consisting of 441 vertices and 800 triangles. The goal is to detect some source points $X_i = (x_i, y_i)$ in Ω having forces $\mathcal{F}_i = (f_i^1, f_i^2), 1 \le i \le N$. At each iteration, a new force is localized on the detected point and its support is represented by a disk of center X_i and radius 0.01. We impose the velocity boundary conditions $u^* = 0$ and $\phi = (0;-2)$ on the boundary of the domain.

We consider two test cases. The first corresponds to the detection of a certain number of source points having forces of the same intensity. The second corresponds to the case of forces of different intensities. Finally, we studied the effect of the distance between two source points on the detection algorithm.

5.1 Source points with the same force

We consider as an example the case of five source points with the same force $\mathcal{F}_i = (1,1)$, $1 \le i \le 5$. Using Algorithm 4.4, we show in Figure 1 the obtained isovalues of δj at each iteration. The obtained exact source point location, corresponding to the minimums found, is given in Figure 2. They represent the exact force point location sought.

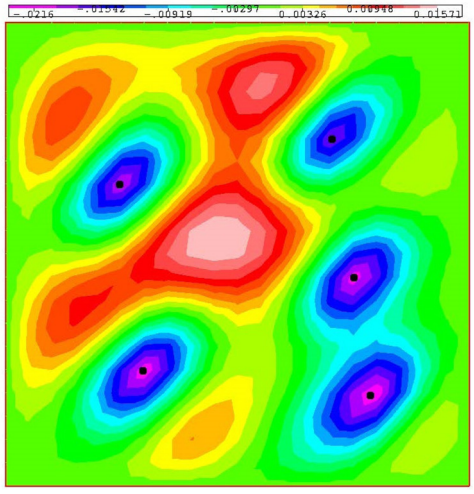

Figure 2: Exact location of the source points (black dots) corresponding to the minimums found after five iterations.

Table 1: Source points location $X_i, 1 \le i \le 5$ and their associated forces

Point source	Location (X_i)	Force ($\mathcal{F}_i$)
1	$x = 0.8,\ y = 0.2$	$\mathcal{F}_x = 1.0, \mathcal{F}_y = 1.0$
2	$x = 0.3,\ y = 0.25$	$\mathcal{F}_x = 1.0, \mathcal{F}_y = 0.0$
3	$x = 0.75,\ y = 0.45$	$\mathcal{F}_x = -1.0, \mathcal{F}_y = -2.0$
4	$x = 0.25,\ y = 0.65$	$\mathcal{F}_x = 0.0, \mathcal{F}_y = -1.0$
5	$x = 0.7,\ y = 0.75$	$\mathcal{F}_x = -1.0, \mathcal{F}_y = 1.0$

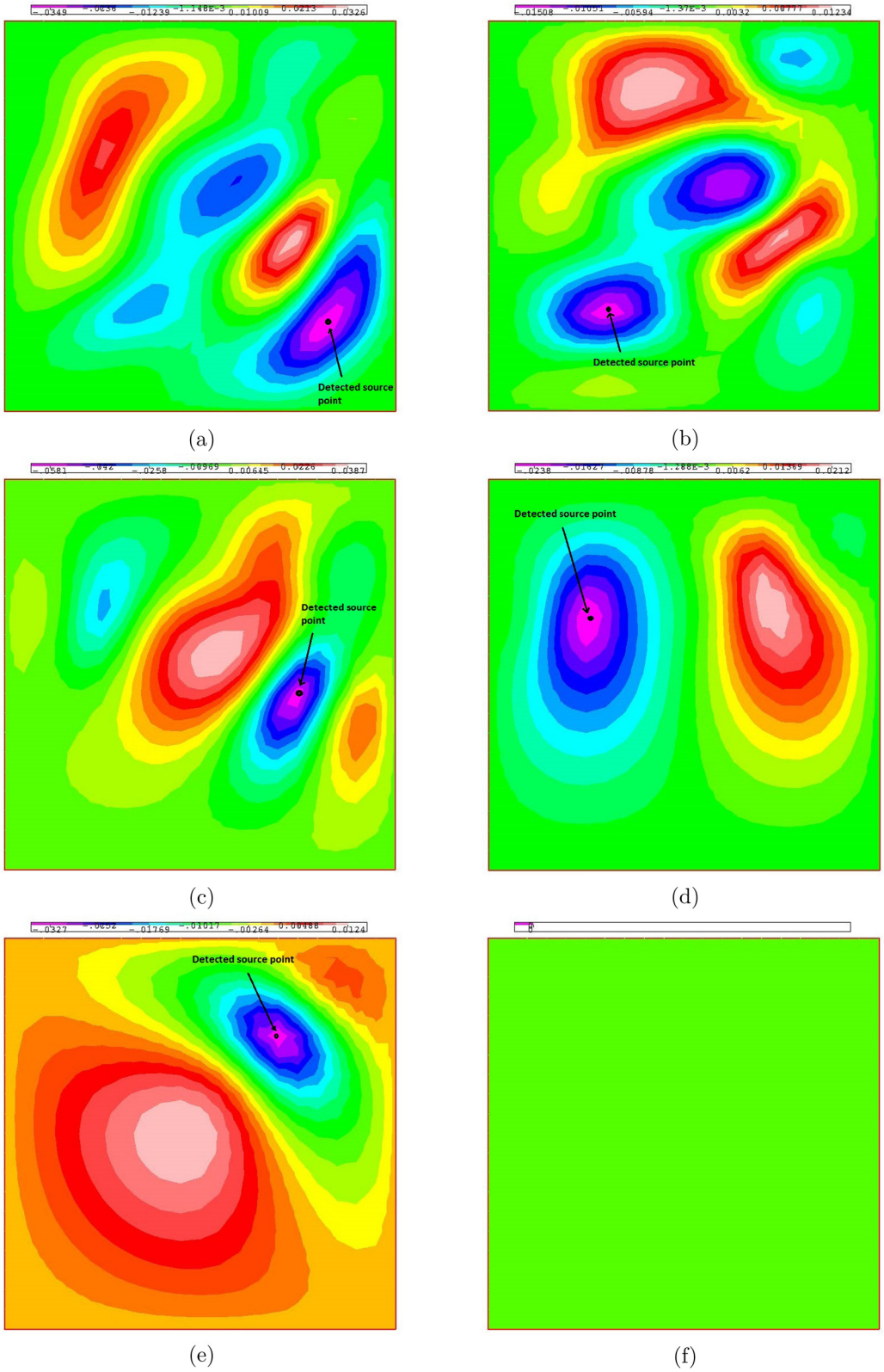

Figure 3: Isovalues of δj showing the exact location corresponding to each global minimum found (black dots): (a) Iteration 1, (b) iteration 2, (c) iteration 3, (d) iteration 4, (e) iteration 5, and (f) iteration 6.

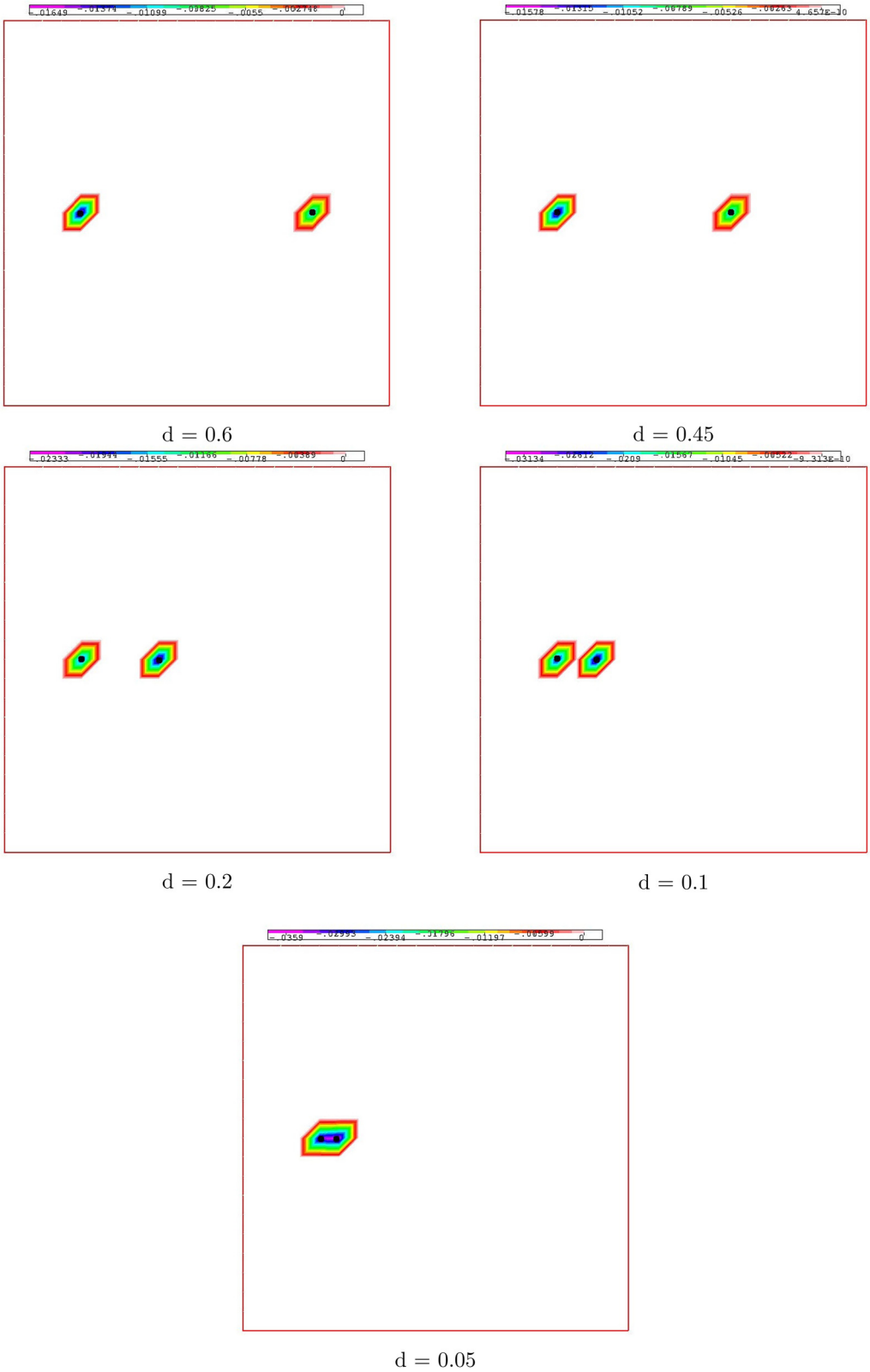

Figure 4: Isovalues of δj showing the exact locations (black dots) and the local minimums (obtained locations) for different values of d.

We remark in Figure 1(f) that the value of δj is positive, which corresponds to the convergence of the algorithm, and confirm that the algorithm determines the exact number of points, taken equal to 5 in the numerical test. In Figure 2, we present all the five source points detected.

Note in this test case that the algorithm used can determine all the source point locations in a single iteration (Figure 1(a)). This was made possible in this case because the forces are equal.

5.2 Source points with different forces

We consider as an example the case of five random source points with different forces $\mathcal{F}_i, 1 \leq i \leq 5$ defined in Table 1. Using Algorithm 4.4, we show in Figure 3 the obtained isovalues of δj at each iteration. The obtained global minimum at each iteration corresponds to one of the exact source point locations.

We remark in Figure 3(f) that the value of δj is positive, which corresponds to the convergence of the algorithm, and confirm that the algorithm determines the exact number of points, taken equal to 5 in the numerical test.

5.3 Effect of the distance between two source points

We study the effect of the distance d, separating two source points, on the identification result.

We consider two source points $s_1 = B(X_1, r)$ and $s_2 = B(X_2, r)$ having the same size $r = 0.02$ and separated by a variable distance d.

For each value of d, we have used Algorithm 4.4 for detecting the corresponding optimal source points location. We present in Figure 4 the isovalues of the obtained δj for different values of d. We show that the exact location, corresponding to the most negative value of δj, can be found when the distance between the two source points decreases until a weak distance between the source points corresponding to the mesh size ($d \geq 0.05$ in this test case). Less than this distance, the algorithm detects only the region containing the two source points, which can be seen as a single “equivalent” one.

6 Comments and conclusion

In this work, a new procedure for the detection of source point location from overspecified boundary data based on minimizing a Kohn-Vogelius-type function is presented. This detection procedure has two main characteristics that make it an interesting method.

The first is its simplicity to be extended to practical situations involving other applications using other partial differential equations such as tumor localization and the detection of wild wells in hydrology.

The second interesting characteristic is the speed and accuracy of the presented algorithm.

This work focuses on the topological sensitivity analysis and its numerical application. Another mathematical question of great interest could be discussed. It corresponds to the detection of source points with incomplete boundary conditions, because several causes can lead to such a situation, in particular when parts of the boundary are not accessible to measurements, or when the boundary conditions cannot be precisely given on them.

Acknowledgment: The authors extend their sincere appreciation to deputyship for Research and innovation, “Ministry of Education” in Saudi Arabia for funding this research (IFKSUOR3-592-1).

Author contributions: All authors have accepted responsibility for the entire content of this manuscript and approved its submission.

Conflict of interest: The authors state that there is no conflict of interest.

Data availability statement: Data sharing is not applicable to this article as no datasets were generated or analyzed during this study.

References

[1] C. Alves and A. Silvestre, *On the determination of point-forces on a Stokes system*, Math. Comput. Simulat. **66** (2004), no. 4, 385–397.

[2] T. Gotz, *Simulating particles in Stokes flow*, J. Comput. Appl. Math. **175** (2005), no. 2, 415–427.

[3] H. Zhou and C. Pozrikidis, *Adaptive singularity method for Stokes flow past particles*, J. Comput. Phys. **117** (1995), no. 1, 79–89.

[4] M. Ouni, A. Habbal and M. Kallel, Determination of point-forces via extended boundary measurements using a game strategy approach, Proceeding of CARI, 2020, pp. 1–8.

[5] M. Abdelwahed and N. Chorfi, *Inverse problem resolution via Khon-vogelius formulation an topological sensitivity method*, Fractals **30** (2022), no. 10, 1–6.

[6] S. Garreau, Ph. Guillaume and M. Masmoudi, *The topological asymptotic for PDE systems: the elasticity case*, SIAM J. Control Optim. **39** (2001), no. 6, 1756–1778.

[7] Ph. Guillaume and K. Sid Idris, *Topological sensitivity and shape optimization for the Stokes equations*, SIAM J. Control Optim. **43** (2004), no. 1, 1–31.

[8] M. Hassine and M. Masmoudi, *The topological sensitivity analysis for the Quasi-Stokes problem*, COCV J. **10** (2004), no. 4, 478–504.

[9] M. Abdelwahed, M. Bensaleh, N. Chorfi and M. Hassine, *An inverse problem study related to a fractional diffusion equation*, J. Math. Anal. Appl. **512** (2022), no. 2, 126–154.

[10] J. Sokolowski and V. Zochowski, *On the topological derivative in shape optimization*, SIAM J. Control Optim. **37** (1999), no. 4, 1251–1272.

[11] M. Abdelwahed and N. Chorfi, *Spectral discretization of the time-dependent Navier-Stokes problem with mixed boundary conditions*, Adv. Nonlinear Anal. **11** (2022), no. 1, 1447–1465.

[12] S. Andrieux and A. Ben Abda, *Identification of planar cracks by complete overdetermined data: inversion formulae*, Inverse Problems **12** (1996), no. 5, 553–563.

[13] A. Friedman and M. Vogelius, *Identification of small inhomogeneties of extreme conductivity by boundary measurements: a theorem on continuous dependence*, Arch. Rat. Mech. Anal. **105** (1989), 299–326.

[14] R. Kohn and M. Vogelius, *Determining conductivity by boundary measurements*, Comm. Pure Appl. Math. **37** (1984), no. 3, 289–298.

[15] M. Jenaliyev, M. Ramazanov, and M. Yergaliyev, *On the numerical solution of one inverse problem for a linearized two-dimensional system of Navier-Stokes equations*, Opuscula Math. **42** (2022), no. 5, 709–725.

[16] J. W. He, Y. Zhou, L. Peng, and B. Ahmad, *On well-posedness of semilinear Rayleigh-Stokes problem with fractional derivative on RN*, Adv. Nonlinear Anal. **11** (2022), no.1, 580–597.

[17] R. Temam, *Navier Stokes equations: Theory and Numerical Analysis*, North-Holland Publishing Company, 1979.

[18] V. Girault and P. A. Raviart, *Finite element methods for Navier-Stokes equations*, Theory and Algorithms, Springer Verlag, Berlin, 1986.

[19] H. Brezis, *Analyse fonctionnelle: Théorie et applications*, Masson, New York, 1983.